International Journal of Advance Research in Science and Engineering
Vol. No.4, Special Issue (01), August 2015
www.ijarse.com
IJARSE
ISSN 2319 - 8354

NUMERICAL INVESTIGATION ON STRUCTURE OF A PARTIALLY PREMIXED METHANE FLAME AT VARIOUS EQUIVALENCE RATIOS

K. B. Sahu[1], P. Ghose[2], Natabar Mohapatra[3], Manas Kumar Puthal[4]

[1]Professor, [2]Asst. Professor, [3,4]M. Tech. Student, School of Mechanical Engineering, KIIT University, Bhubaneswar, (India)

ABSTRACT

A numerical investigation on the prediction of temperature, major species (CH_4, CO_2, CO, H_2O, N_2, O_2) from methane/air partially premixed flames are obtained for different primary equivalence ratios (ϕ). A computational model for an axi-symmetric partially premixed flame has been developed. Standard k-ε model is used to simulate the turbulent quantities. Different species transport equations are solved for different species followed by Fick's law. In order to predict the soot, Brookes and Moss soot model has been incorporated along with modified model constants through a developed precursor correlation. Discrete ordinate (DO) radiation model is employed to include the radiation effect throughout the flow field. The governing equations are solved by using ANSYS Fluent 14.0. The pressure based steady solver has been used to solve 2-D geometry in Cartesian co-ordinate system. When the equivalence ratio increases, the flame height observed to increase. The exact flame height is ascertained from the axial distributions of temperature and different species. The soot in the flame of equivalence ratio ϕ=1.48 is negligibly small and distributed in a very small area along the axis. The formation of soot in the flames is higher with increase in equivalence ratio.

Keywords: Equivalence ratio, Partially premixed flames, Soot, Species.

I. INTRODUCTION

A partially premixed flame is formed when a rich mixture of fuel and air in a primary stream interacts with a lean mixture of fuel and air or air only in secondary stream. When correct premixing conditions are placed, then the partially premixed flames creates a lesser amount of pollution and are more steady. Several examples are present in the field of partially premixes flames such as, industrial furnaces, flames in gas turbine combustion chambers, spray flames, direct injection automobile engines, Bunsen flames, etc. Modern gas turbine combustion systems originally manufactured for non-premixed mode of combustion is prone to partial premixing due to geometric features are the best example for this kind. Partial premixed mode has advantage over non-premixed and premixed modes. Non-premixed combustion regime has the drawback of attaining high temperatures which effects the emission formation like NO. On the other end, lean premixed combustion is prone to generate combustion instabilities with high pressure fluctuations. Many works have been carried out with methane as the fuel in gaseous partially premixed flames. Because, methane has the large contribution to the natural gas for the practical applications. T. K. Mishra et al. [1] have experimentally investigated the species

concentration distribution in a partially premixed methane/air flame established on a axi-symmetric coaxial burner. The flame structures of laminar partially premixed flames of two different fuels (methane and propane) have also been compared by them [2]. Gore and Zhan [3] have experimentally investigated the NO_x emission and concentration of major species in a laminar partially premixed flame taking methane as the fuel in a co-flow central tube burner. The temperature and CO concentrations have been measured by Datta et al. [4] in a methane partially premixed flame in a co-flow burner using Coherent Anti-strokes Raman Scattering (CARS) method. Mokhov and Levensky [5] have measured temperature and the NO concentration in the burnout area of a methane partially premixed flame in a co-flow ceramic burner with upstream heat loss by using techniques of CARS and LIF respectively. Six co-flowing laminar, partially premixed methane/air flames have been investigated computationally and experimentally [6] to determine the fundamental effects of partial premixing by varying the primary equivalence ratio from ∞ (nonpremixed) to 2.464. Claramount et al [7] have analyzed, by means of detailed numerical simulations, the influence of the partial premixing level and the adequacy of different mathematical submodels on the modelling of co-flow partially premixed methane–air laminar flames. The partially premixed methane/air flame have been investigated by Gicquel [8] in a two-dimensional configuration. The configuration was close to those used in real domestic boilers. Bennet et al [9] have studied on six co-flowing laminar ethylene/air flames, by varying the primary equivalence ratio from infinity (nonpremixed) to 3, to determine the fundamental effects of partial premixing. In the present work, five methane/air partially premixed flames of various equivalence ratios and a methane non-premixed flame are investigated to study the effect of equivalence ratios on the temperature and major species (CH_4, CO_2, CO, H_2O, N_2, O_2) distribution. Two partially premixed flames of same equivalence ratio and different primary jet velocities are considered to study the influence of jet velocity.

II. SPECIFICATION AND GEOMETRY OF THE PROBLEM

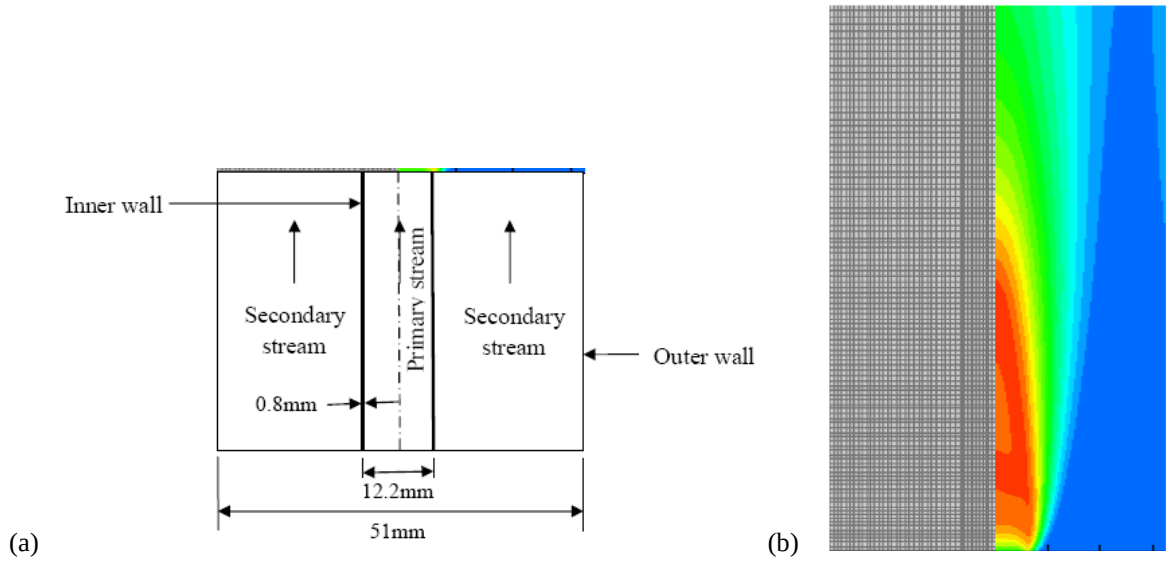

Figure 1. (a) Physical and (b) Meshed Computational Domain

2.1 Physical and Computational Domain

Fig. 1 shows the physical and meshed computational domain for the combustion in an axi-symmetric burner. The internal tube is of diameter 12.2 mm and thickness 0.8 mm where as the outer tube is of 51 mm diameter. The fuel-air mixture enters through the inner tube and secondary air flows through the outer annular space. The flame is produced above the burner. As the physical domain is symmetrical about the axis if the burner, the computational domain is taken half of the physical domain.

2.2 Operating Conditions and Boundary Conditions

In the present work, six flames have been studied. The operating condition of each flame is tabulated in TABLE 1. The first five flames are partially premixed flame where as the sixth flame is a non-premixed flame. The required fuel and air velocities to achieve these operating conditions are tabulated in TABLE 2.

The outer surface is assumed to be the adiabatic wall with no slip condition. At the entrance of the inner tube, the primary jet velocity is given as the velocity inlet to that face. At the outlet, the atmospheric pressure is given as the pressure boundary condition. Similarly, the secondary velocity is given as the velocity inlet to the appropriate face.

Table 1. Operating Conditions

Run No.	Fuel flow rate (l/min)	Primary premixing air flow rate (l/min)	Secondary co-flow air flow rate (l/min)	Primary jet velocity (m/s)	Secondary velocity (m/s)	Primary equivalence ratio
1	0.56	3.6	40	0.5931	0.3521	1.48
2	0.56	3.0	40	0.5075	0.3521	1.77
3	0.56	2.5	40	0.4362	0.3521	2.13
4	0.56	1.7	40	0.3222	0.3521	3.14
5	0.9	2.73	40	0.5175	0.3521	3.14
6	0.56	0	40	0.0798	0.3521	∞

Table 2. Boundary Conditions for ANSYS Fluent

Run No.	Inlet Air Velocity (m/s)	Inlet fuel Velocity (m/s)	Mass fraction of CH_4	Mass fraction of O_2	Primary Equivalence Ratio
1	0.3521	0.5971	0.077621	0.212147	1.48
2	0.3521	0.5075	0.091721	0.208904	1.77
3	0.3521	0.4362	0.108033	0.205141	2.13
4	0.3521	0.3222	0.151252	0.195212	3.14(0.56)
5	0.3521	0.5175	0.151353	0.195189	3.14(0.9)
6	0.3521	0.0798	1	0	∞

Turbulent intensity = 5 %

Turbulent length scale (m) = 0.00357 m

International Journal of Advance Research in Science and Engineering
Vol. No.4, Special Issue (01), August 2015
www.ijarse.com
IJARSE
ISSN 2319 - 8354

III. RESULT AND DISCUSSIONS

The species and temperature distribution within a partially premixed flame depends on the equivalence ratio of fuel air mixture and the velocity of the mixture. In the present study different partially premixed flames and a nonpremixed flame are taken to see the species and temperature distribution within the flame. The results are obtained and discussed as follows:

3.1 Temperature Contours

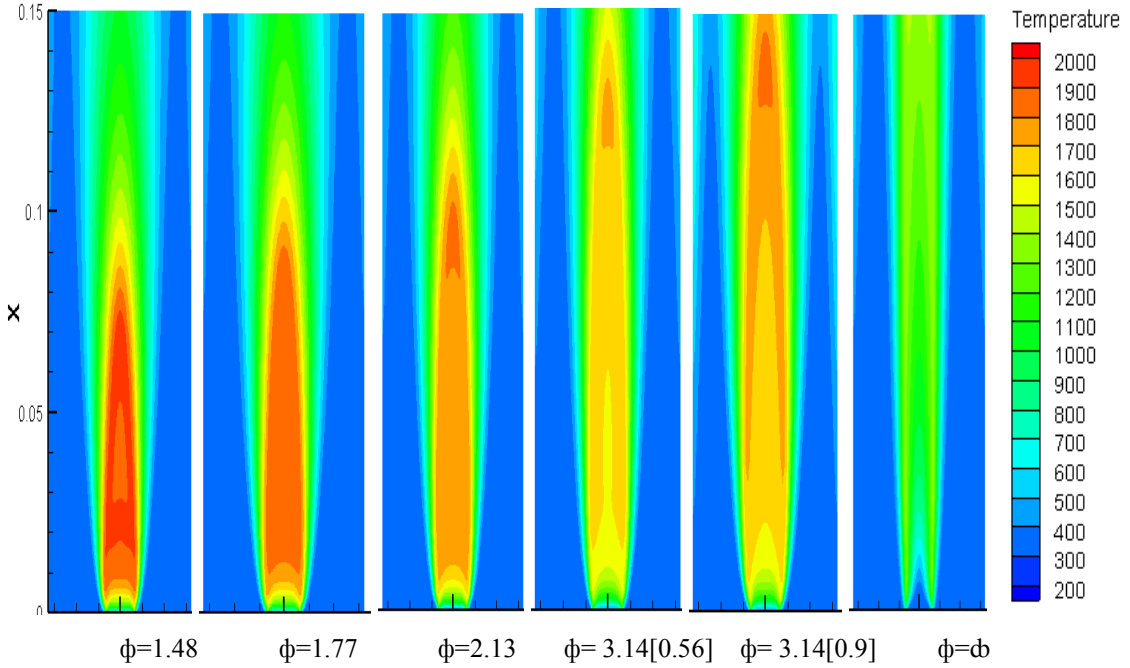

Figure 2. Temperature Contours for Flames for Different Equivalence Ratios

Fig. 2 shows the temperature contours of flames for different equivalence ratios. When the equivalence ratio increases, the flame height is observed to increase. The exact flame height is ascertained from the axial distributions of temperature and different species. The flame height is less for flames having smaller equivalence ratio, because the reaction zone is developed early as more oxygen is available in the mixture. The fuel is consumed within a smaller distance from the burner exit. The premixed flame having least equivalence ratio has reached the maximum temperature.

Two cases (run 4 and 5) having same primary equivalence ratio ϕ=3.14 with different inlet velocity have been considered to study the effect of velocity on structure of the flames. To keep the equivalence ratio same with different primary jet (air-fuel mixture jet) velocity, the fuel flow rate and the primary air flow rate have been varied. For the flame with the higher primary jet velocity, the flame height and the temperature are more compared to the other flame.

A special case of purely diffusion flame (run 6) has also been taken. The height of this flame is much longer compared to the premixed flames and the tip is not observed within the computational domain. The temperature of this flame is lowest among all the flames.

3.2 Soot Contours

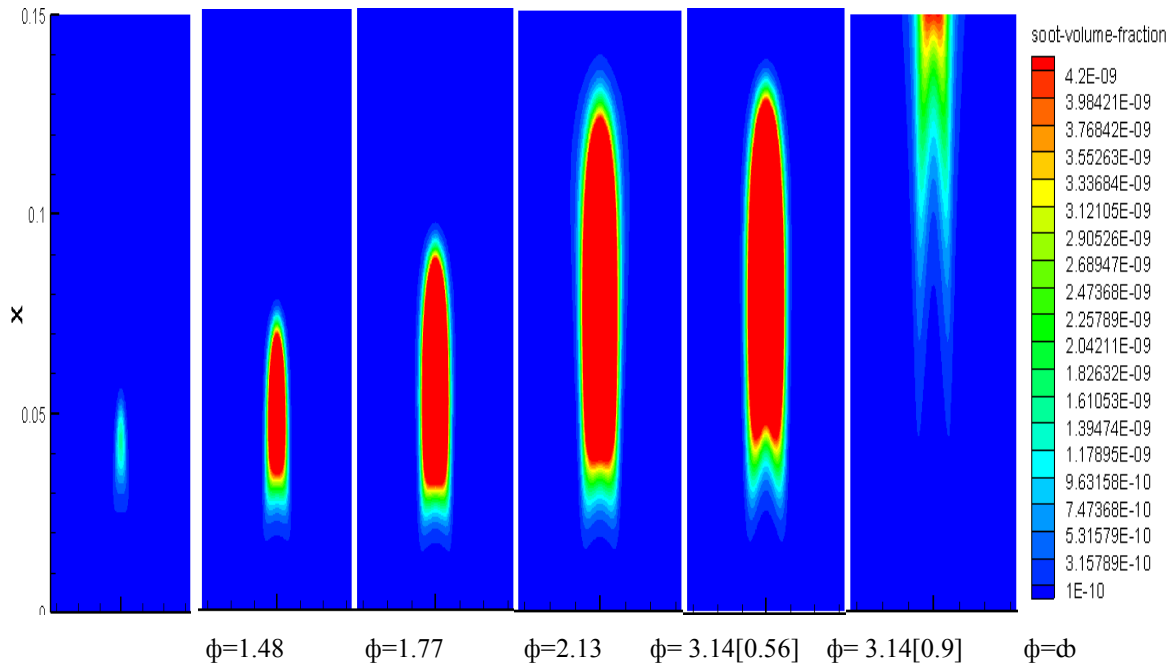

Figure 3. Contours of Soot in the Flames of Different Equivalence Ratios

Contours of soot for different flames are shown in Fig. 3. The soot in the flame of equivalence ratio ϕ=1.48 is negligibly small and distributed in a very small area along the axis. The soot formation in flames increases with equivalence ratio. Between the two flames having same equivalence ratio, the soot developed in the flame having smaller jet velocity is slightly more. The soot formed in nonpremixed flame is not obtained fully as the entire flame is not within the computational domain considered.

3.3 Temperature Variation Along the Axis

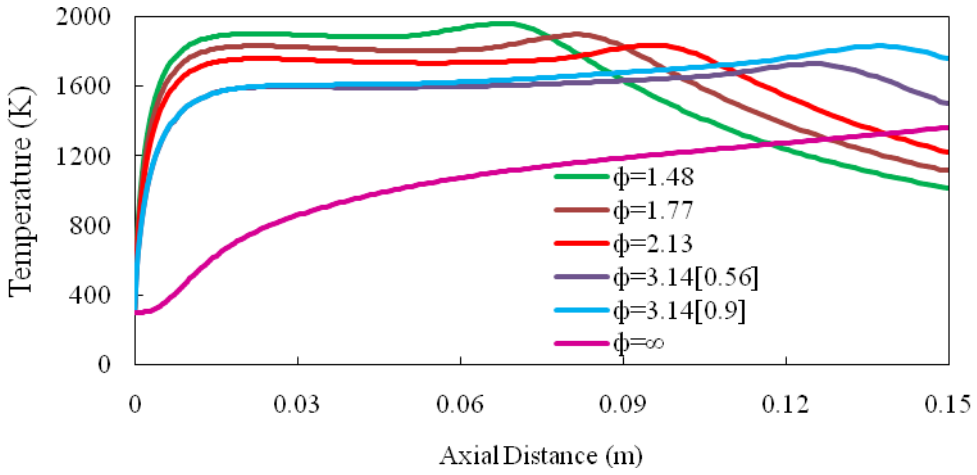

Figure 4. Axial Temperature Distribution for Different Equivalence Ratios

Fig. 4 depicts the temperature variation along the axis of the burner. For all the flames, the temperature at the exit of the burner is same as the atmospheric temperature at which the fuel air mixture enters. Further downstream, the axial temperature increases rapidly from atmospheric temperature as the heat is diffused from

the flame front towards the axis. The temperature increases to the maximum at a certain axial distance where the tip of the flame is located. Further downstream, the temperature decreases because heat is diffused radially outwards.As the equivalence ratio increases, the peak axial temperature is located at a higher distance from the burner exit. This means the flame height is more for higher equivalence ratios. This is also evident from the temperature contours of all the flames (Fig. 2). The overall temperature of the flames is less for lower equivalence ratios. This is because, for flames of lower equivalence ratios, the soot developed in the flames is low (Fig. 3) and less heat is radiated away from the flame. The flame height is smaller for low equivalence ratios and axially stretched more for higher equivalence ratios which is evident from the axial temperature distribution (Fig. 4) as well as from temperature contours (Fig. 2) of different flames. This is because, at lower equivalence ratio, as the stoichiometric condition is reached early after diffusion of oxygen from the secondary stream, the reaction zone is closer to the inlet. For two flames with same equivalence ratio and different velocities, the temperature along the axis is almost same near the burner exit, but at the downstream, the temperature is more for the flame having higher primary jet velocity. This is because of the stretching of the flame height due to higher jet velocity.

For the case of purely diffusion flame, it is observed that for some distance from the burner exit, the temperature does not increase (Fig. 2 and 4) and it gradually increases downstream. At the burner exit, due to absence of air, no combustion can take place. But further downstream, as air is diffused from the secondary stream, the combustion commences and the temperature increases. As only fuel comes through the primary stream, it takes more time to consume the fuel downstream for which the flame is stretched much more beyond the computational domain adopted here. The axial temperature of this flame is the lowest of all as most of the heat is absorbed by the excess fuel.

3.4 Radial temperature distribution at different heights

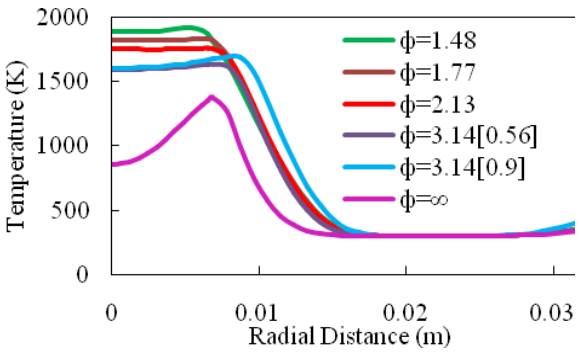

Figure 5. Radial temperature distribution at a flame height of 0.03 m

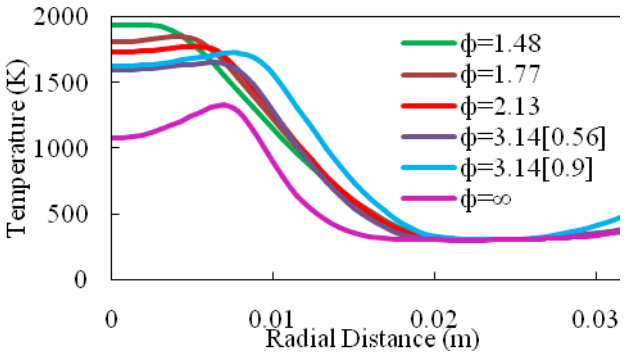

Figure 6. Radial temperature distribution at a flame height of 0.06 m

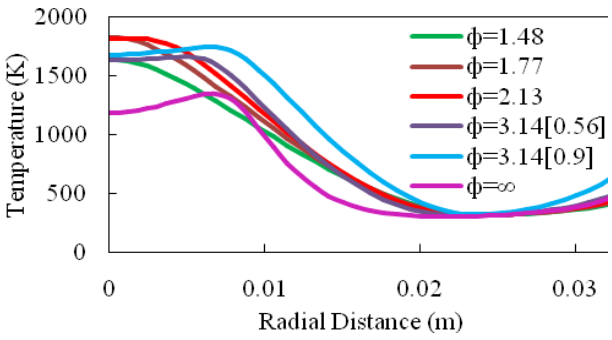

Figure 7. Radial temperature distribution at a flame height of 0.09 m

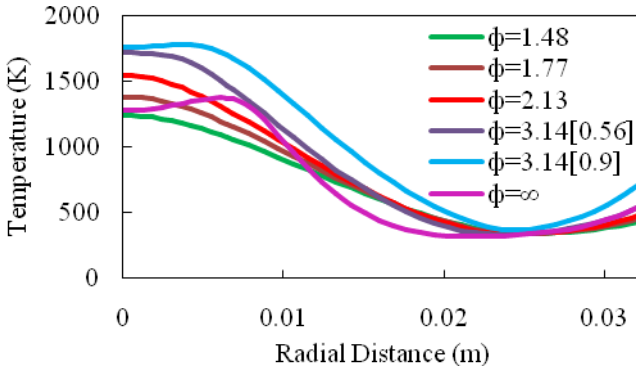

Figure 8. Radial temperature distribution at a flame height of 0.12 m

Fig. 5 shows the radial temperature distribution of flames for different equivalence ratios at a height of 0.03 m from the burner exit. For all flames, as we approach from the outer wall of the burner along radial direction towards the axis, the temperature is constant within the region where secondary air flows at atmospheric temperature. The temperature is somewhat higher near the wall as heat is transferred from the wall to the adjacent layer. As we further approach towards the axis the temperature is gradually increased to a maximum. This is the location where nonpremixed flame is produced. Then the temperature remains almost constant up to the axis of burner. As explained earlier, the flames are stretched more as equivalence ratios is increased. The width of the flame is less for lower equivalence ratios which is also evident from the plot. But the temperature of the flame near the axis is higher for flames of lower equivalence ratios as the stoichiometric condition is reached early. Between the two flames having same equivalence ratios and different primary velocities, the flame having higher primary velocity is stretched more for which the peak temperature is at a higher radial distance compared to the other. For the diffusion flame, the flame is narrow at this height as the flame is extended beyond the computational domain which is explained earlier. This is also observed from the peak temperature of the flame. The temperature is reduced from the peak towards the axis as the heat is absorbed by the fuel flowing in the primary stream. Fig. 6 shows the radial temperature distribution of all flames at a height of 0.06 m from the burner exit. Similar result is also observed here as that obtained at a height of 0.03 m. But the temperature near the wall is increased further since the wall temperature is increased downstream. The width of the flames is observed to be less as flames are closed ones. The difference in temperature of the diffusion flame at the peak and that towards the axis has become less as heat is absorbed by the fuel in the primary stream as it flows downstream. Fig. 7 shows the radial temperature distribution of all flames at a height of 0.09 m from the burner exit. For the flame with lowest equivalence ratio taken in our study, the peak temperature is observed at the axis. So at this height (0.09 m) the tip of the flame is located. Since the stoichiometric condition for other flames is reached after that for the flame of lowest equivalence ratio, the temperature and width of these flames are more. Also as the width of these flames is increased and more heat is transferred from the wall to the secondary air the flat portion of the plot in the secondary air region has become negligible. Fig. 8 shows the radial temperature distribution of all flames at a height of 0.12 m from the burner exit. At this height, the peak temperature of the flame having equivalence ratio 2.13 is observed at the axis. So the tip of this flame is located at this height. So it is obvious that the tip of the flame having equivalence ratio 1.77 is located between 0.09m and 0.12 m. The

temperature of the flames is higher for higher equivalence ratios. Also the temperature of secondary air is increased due to heat received from both sides.

3.5 Axial Distribution of Different Species in a Flame

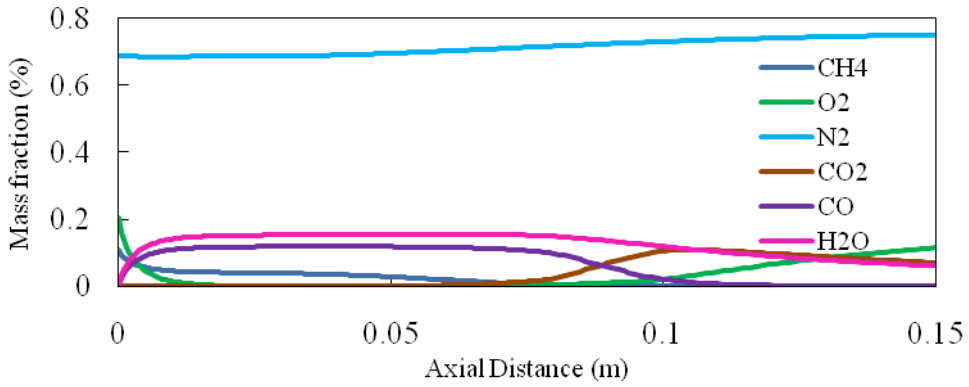

Figure 9. Species Mass Fraction Distribution Along the Axis at ϕ = 2.13

Fig. 9 shows the axial distribution of mass fraction of all species in the flame at equivalence ratio (ϕ) = 2.13. It is clearly observed that, the mass fraction of methane (CH_4) is the maximum at the exit of the burner and it decreases rapidly within a small distance and then decreases slowly downstream. The flame front is produced at some radial distance from the axis and as fuel is consumed there, the fuel is diffused from the primary stream towards the flame front. The decrease in mass fraction of CH_4 is rather slow afterwards and finally reduces to zero at the tip of the flame. Similarly oxygen is also transported from the primary stream to the flame front and the mass fraction decreases near the inlet towards downstream. However oxygen mass fraction along the axis again increases after reaching to the minimum at the flame tip. It is because beyond the flame tip, oxygen in the secondary air is diffused towards the axis. If we focus on the distribution of CO_2, it is found that, there is no CO_2 mass fraction nearly up to the flame tip. The concentration of CO_2 suddenly increases around the flame tip because of formation of CO_2 at the flame tip. Then mass fraction of CO_2 decreases downstream as it diffuses along radial direction towards the secondary stream. Regarding axial distribution of H_2O and CO concentration, it increases rapidly at the inlet, then remains constant up to the tip of the flame. The H_2O and CO are formed at the flame front and diffused towards the axis. At the inlet concentration of these species is zero for which the diffusion is rapid. After the concentration reaches to a value so that the diffusion of these species is not possible (when equalises with the concentration at the flame front), the concentration along the centreline remains constant up to the flame tip. The concentration of H_2O decreases gradually beyond the flame tip due to radial diffusion whereas the concentration of CO decreases to zero as it is consumed entirely at downstream by reacting with excess air present. N_2 concentration remains same within the flame and gradually increases from the flame tip to the outlet, because the N_2 present in the secondary stream is diffused towards the axis. The axial distribution of all the species for different equivalence ratios are observed to be similar in nature, but the magnitude of concentrations are different which is explained in the following section.

3.6 Axial Distribution of Species in Different Flames

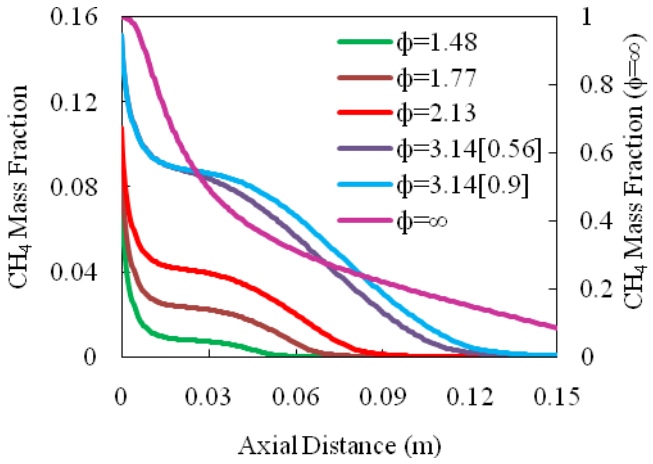

Figure 10. Axial distribution of CH_4 in different flames

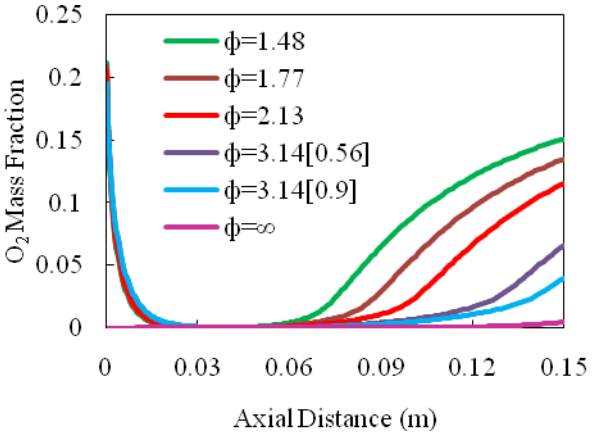

Figure 11. Axial distribution of O_2 in different flames

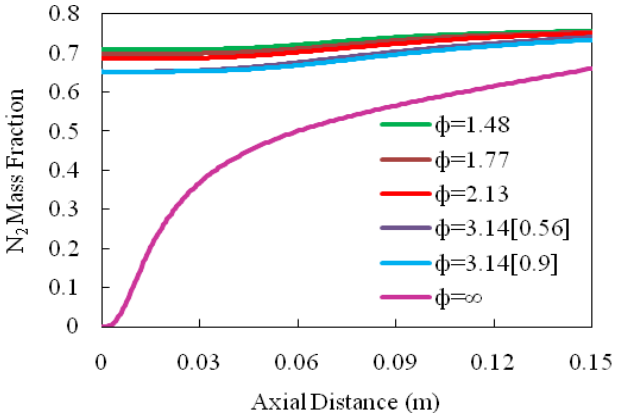

Figure 12. Axial distribution of N_2 in different flames

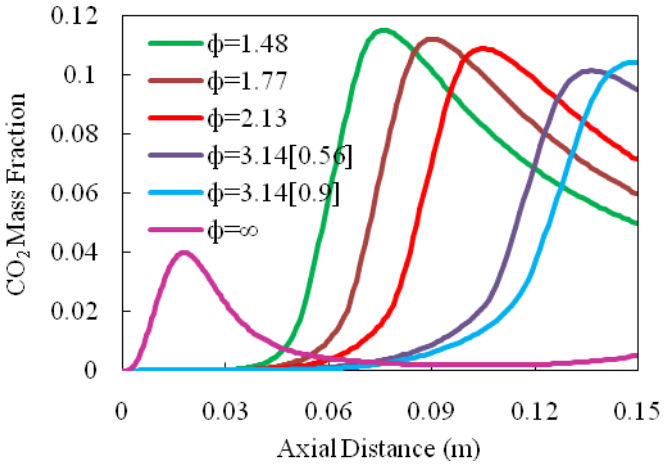

Figure 13. Axial distribution of CO_2 in different flames

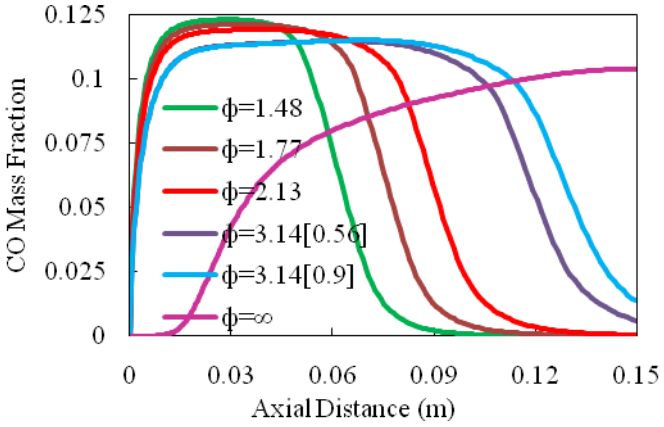

Figure 14. Axial distribution of CO in different flames

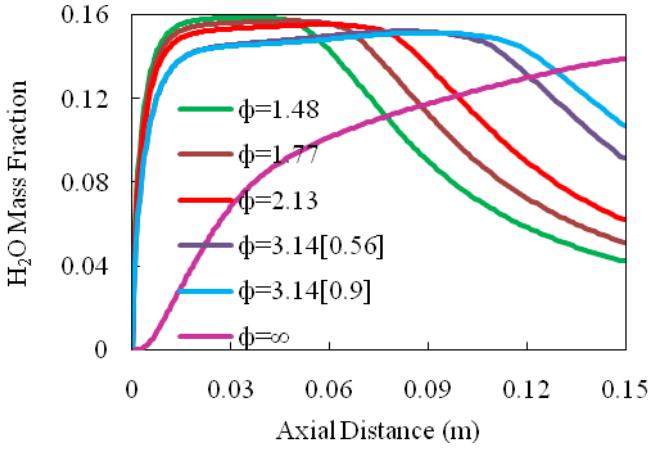

Figure 15. Axial distribution of H_2O in different flames

Axial distribution of methane for different flames is shown in Fig. 10. At the burner exit, the mass fraction of methane is minimum for ϕ = 1.48 and it is more for other flames as the equivalence ratio is increased. For the nonpremixed flame the mass fraction is maximum (=1) as the primary stream contains only fuel. Along the axial

direction the mass fraction decreases to zero at the flame tip as explained earlier. Since the flame height is more as equivalence ratio increases, the axial location at which mass fraction of the fuel becomes zero is accordingly located. Since the tip of the nonpremixed flame is not located within the computational domain, the mass fraction continuously decreases from the inlet up to the outlet, but has not reached to zero. Fig. 11 shows the axial distribution of oxygen for different flames. At the inlet the mass fraction of oxygen for ϕ= 1.48 is more and it decreases for flames of higher equivalence ratios. As the difference in mass fraction of oxygen at the inlet is very less, it is not distinguishable from the plot. The concentration of oxygen then decreases to almost zero up to the flame tip and increases thereafter. Since the flame height is different for the flames, the location is observed accordingly. The mass fraction of oxygen along the axis is negligible throughout the computational domain. The axial distribution of nitrogen mass fraction is shown in Fig. 12. For all the premixed flames the mass fraction of N_2 is almost same as there is no consumption of nitrogen at the flame front and there is no diffusion of nitrogen from the axis towards the flame front. The slight increase in N_2 concentration downstream may be attributed to diffusion of N_2 from the secondary stream towards the axis. Though the difference of mass fraction for different flames is very small, the concentration is higher for low equivalence ratio flames throughout the length. Fig. 13 shows axial distribution of CO_2 mass fraction for different flames. For all the premixed flames no CO_2 is observed up to the flame tip and the concentration is suddenly increased at the flame tip and then decreases gradually. As the flame height is different for different flames, the location where concentration of CO_2 increases suddenly is observed accordingly. For the nonpremixed flame, the concentration of CO_2 first increases from the inlet to a peak value and then decreases continuously up to the outlet. Fig. 14 shows the axial distribution of CO for different flames. For different premixed flames the concentration of CO is rapidly increased near the inlet and then remains constant up to the flame tip. Then it decreases to zero beyond the flame tip. As the flame height is different for different flames, the locations of flame tip are observed accordingly. For the diffusion flame, there is no concentration of CO for certain distance near the inlet and the concentration increases gradually up to the outlet. Fig. 15 shows the axial distribution of H_2O of all flames. For all premixed flames, the concentration of H_2O increases rapidly near the inlet and remains constant up to the flame tip and gradually decreases thereafter up to the outlet. For the nonpremixed flame, the concentration of H_2O increases continuously but slowly up to the outlet.

3.7 Radial Distribution of Species and Temperature in the Flame (ϕ = 2.13)

Fig. 16 shows the radial distribution of different species and temperature at a height of 0.03 m from the burner exit for the flame of equivalence ratio ϕ = 2.13. The concentration of methane remains constant from the axis to the flame front where the fuel is consumed. So the concentration of fuel deceases gradually to zero which continues outwards as there is no fuel in the secondary stream. The concentration of oxygen in the secondary stream is maximum and same from the outer wall up to the flame front. It is consumed there for which the concentration gradually decreases and the concentration is negligibly small up to the axis.

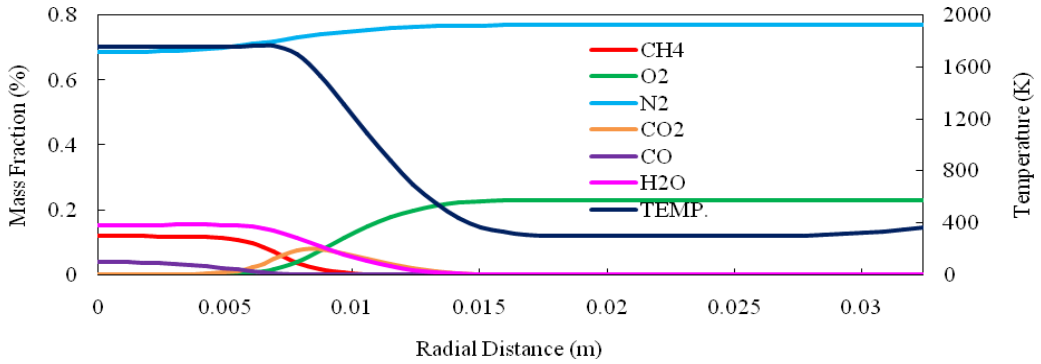

Figure 16. Radial Distribution of Species and Temperature for the Flame (ϕ = 2.13) at a Height of 0.03 m

The trend of nitrogen concentration is similar to that of oxygen. But the concentration of nitrogen from the flame front up to the axis is slightly less than that in the secondary stream as there is no consumption of nitrogen in the flame front. The concentration of CO_2 peaks at the flame front and decreases on either side because the CO_2 formed at the flame front is diffused to both sides. The CO concentration from the axis to the flame front almost remains same as CO is formed within the flame due to insufficient oxygen there. At the flame front CO is converted to CO_2 as oxygen is diffused from the secondary stream to the flame front. The concentration of H_2O is uniform within the flame as it is produced there. There is no concentration of H_2O in the secondary zone since no oxygen present in the secondary stream. So the concentration of H_2O is decreased gradually at the flame front as we move radially outward. The temperature is maximum within the flame and the magnitude is around 1760K as combustion occurs there. The temperature is gradually decreased to the ambient temperature of 300K in the secondary stream. The temperature is somewhat increased near the wall as some heat is transferred from the wall to the air.

IV. CONCLUSION

- ✓ The flame height increases with increase in equivalence ratio.
- ✓ The formation of soot in the flames is higher with increase in equivalence ratio.
- ✓ The temperature increases to the maximum at a certain axial distance where the tip of the flame is located. Further downstream, the temperature decreases because the heat is diffused radially outward. As the equivalence ratio increases, the peak axial temperature is observed to be at a higher distance from the burner exit.
- ✓ The wall temperature increases with increase in equivalence ratio throughout the length of burner. At lower equivalence ratio the soot formation is less and it increases with increase in equivalence ratio.
- ✓ For all flames, as we approach from the outer wall of the burner along radial direction towards the axis, the temperature is constant within the region where secondary air flows which is at atmospheric temperature. The temperature is somewhat higher near the wall as heat is transferred from the wall to the adjacent layer.
- ✓ For the diffusion flame, the flame is narrow at this height as the flame is extended beyond the computational domain.
- ✓ The mass fraction of methane (CH_4) is the maximum at the inlet of the burner and it decreases rapidly within a small distance and then decreases slowly along the axis downstream.

- ✓ Similarly oxygen (O_2) is also transported from the primary stream to the flame front and the mass fraction decreases at the inlet towards downstream.
- ✓ N_2 concentration remains same within the flame and gradually increases from the flame tip to the exit, because the N_2 present in the secondary stream is diffused towards the axis.
- ✓ We focus on the distribution of CO_2, it is found that, there is no CO2 mass fraction nearly up to the flame tip.
- ✓ The H_2O and CO are formed at the flame front and diffused towards the axis. At the inlet concentration of these species is zero for which the diffusion is rapid.
- ✓ At ϕ =2.13, The temperature is maximum within the flame and the magnitude is around 1760K as combustion occurs there. The concentration of methane remains constant from the axis to the flame front. The concentration of oxygen in the secondary stream is maximum and same from the outer wall up to the flame front.

REFERENCES

[1] T. K. Mishra, A. Datta, A. Mukhopadhaya, "Concentration measurements of selected hydrocarbons in methane/air partially premixed flames using gas chromatography", International Journal of Thermal Sciences vol. 44, pp. 1078-1089, 2005.

[2] T. K. Mishra, A. Datta, A. Mukhopadhaya, "Comparison of the structures of methane-air and propane-air partially premixed flames", Fuel, vol. 85, pp. 1254-1264, 2006.

[3] J. P. Gore and N. J Zhan, "NO emission and major species concentrations in partially premixed laminar methane/air co-flow flames", Combustion Flame, vol. 105, pp. 414-417, 1996.

[4] Datta, F. Beyrau, T. Seeger, A. Leipertz, "Temperature and concentration measurements in a partially premixed CH4/air coflowing jet flame using coherent anti-strokes raman scattering", Combustion Science Tech, vol. 176 (11), pp. 1965-1984, 2004.

[5] V. Mokhov, H. B Levensky, "NO formation in the burnout region of a partially premixed methane/air flame with upstream heat loss", Combustion and Flame, vol. 118, pp. 733-740, 1999.

[6] A. V. Bennet, C. S. Mcenally, L. D. Pfeffrle, M. D. Smooke, "Computational and experimental study of axisymmetric coflow partially premixed methane/air flames", Combustion and Flame, vol. 123, pp. 522-546, 2000.

[7] K. Claramunt, R. Consul, C. D. P. Segarra, A. Oliva, "Multidimensional mathematical modeling and numerical investigation of coflow partially premixed methane/air laminar flames", Combustion and Flame, vol. 137, pp. 444-457, 2004.

[8] O. Gicquel, P. Miquel, V. Quilichini, M. Hilka, D. Thevenin, N. Darbha, "Numerical and experimental study of NO emission in laminar partially premixed flames", Proceedings of the Combustion Institute, vol. 28, pp. 2419-2425, 2000.

[9] B. A. V. Bennet, C. S. Mcenally, L. D. Pefferle, M. D. Smooke, "Computational and experimental study of axisymmetric coflow partially premixed ethylene/air flames", Combustion and Flame, vol. 127, pp. 2004-2022, 2001.